Journal of Applied Polymer Science

Photo/pH dual-responsive biocompatible poly(methacrylic acid)-based particles for triggered drug delivery

Lili Yu,[1,2] Ning Ren,[1] Kuan Yang,[1] Miao Zhang,[1] Li Su[1]
[1]Department of Pharmacy, Xi'an Medical University, Xi'an, Shaanxi 710021, China
[2]Stake Key Laboratory of Natural and Biomimetic Drugs, Peking University, Beijing 100191, China
Correspondence to: L. Yu (E-mail: yulili0218@163.com)

ABSTRACT: A novel dual-responsive (light and pH) particle based on poly(methacrylic acid), poly(methacrylic acid)–poly[1-(2-nitrophenyl)ethane-1,2-diyl bis(2-methylacrylate)]was prepared with the facile method of two-step homogeneous radical polymerization with methacrylic acid as the monomer and 1-(2-nitrophenyl)ethane-1,2-diyl bis(2-methylacrylate) as a photodegradable crosslinker. Photolytic assessments were conducted upon irradiation with a UV lamp; this led to particle disintegration caused by cleavage of the photolabile crosslinking points. The light-dependent degradation was investigated through particle size changes, absorption spectra variations, surface morphology changes, Fourier transform infrared spectroscopy, and the release of Nile red from the particles after irradiation. The pH dependence of the particle systems induced by the protonation and deprotonation of poly(methacrylic acid) was also confirmed by fluorescence spectroscopy. The triggered release of fluorescein diacetate was investigated to demonstrate that the release behavior in cells was light dependent. © 2016 Wiley Periodicals, Inc. J. Appl. Polym. Sci. **2016**, *133*, 44003.

KEYWORDS: biomaterials; crosslinking; photochemistry; stimuli-sensitive polymers

Received 27 October 2015; accepted 1 June 2016
DOI: 10.1002/app.44003

INTRODUCTION

Drug-delivery systems that can prevent the leakage of the encapsulated compound at the targeted site or at specific time points have attracted much attention.[1] To realize this aim, many efforts have been directed toward the development of carriers that respond to certain triggers, such as pH,[1–4] temperature,[5,6] redox,[3,7–10] specific enzymes,[11] and light.[1,10,12–20] Some of the efforts have been directed toward the development of intelligent carriers that respond to single stimuli, such as temperature, pH, ionic strength, and light.[1,3,10]

In view of the previous challenges, one approach for obtaining on-demand drug release is the combination of two or more internal triggers, such as temperature, pH, redox, and others, in one series of particles.[21] For instance, Luo *et al.*[21] developed dual-responsive micelles that responded to *cis*-diol and pH for on-demand drug release at the target site for cancer treatment. However, compared with delivery that is responsive to two internal stimuli, a strategy with both external stimuli (e.g., pH, redox, and specific enzymes) and internal stimuli (e.g., temperature and light) is much more attractive because of the more controllable and effective drug-release process that can be achieved through the adjustment of the intensity and duration of the external stimulus.[10,22–24] With respect to this point, photoresponsive drug carriers, widely investigated in dual-responsive strategies because the use of light as an external stimulus is a clean, rapid, and precise method.By controlling the wavelength and intensity, one can accurately control the light remotely and accurately; it can be quickly switched and easily focused on specific areas with high triggering efficiency.[15,22,25] For example, Yu *et al.*[18] developed hybrid pH/near-infrared light dual-responsive micelles, and their on-demand drug-release process was demonstrated. Meng *et al.*[20] prepared pH/light dual-responsive crosslinked polymeric micelles by the self-assembly of crosslinked amphiphilic glycol chitosan−*o*-nitrobenzyl succinate conjugates, and *in vitro* evaluation showed that a hydrophobic drug could be quickly released at low pH with light irradiation.

Photoresponsive particles containing *o*-nitrobenzyl have been used in many studies because the reaction of these chromophores is fast and can be quantitatively controlled with UV irradiation.[1] Zhao and coworkers[26–29] have been pioneers in the development of *o*-nitrobenzyl containing particles for potential drug delivery. Moreover, to achieve on-demand drug release at a targeted site or at a certain time point, Zhao's group has synthesized *o*-nitrobenzyl containing multiresponsive particles

Additional Supporting Information may be found in the online version of this article

bearing a redox-cleavable unit and a photocleavable unit.[10] Additionally, in a previous study, we reported the design and formation of carriers containing a photolabile *o*-nitrobenzyl unit, and we demonstrated that the rapid breakdown and deformation of carriers upon irradiation with UV light can result in the dumping of the encapsulated molecules.[12,14,15]

In addition, pH has frequently been used as an internal trigger in the area of dual stimuli-responsive particles.[3,25] Smart particles may degrade or expand because of pH level variation in the microenvironment.[1] Thus, such concepts are currently being investigated to control the drug-release process through the exploitation of the lower pH level of lysosomes and tumor tissue.[30] The pH dependence of particles for drug delivery usually involves moieties that can protonate and deprotonate at different pH levels.

Herein, considering the previous issues, we report the design and fabrication of a novel dual (light/pH) responsive smart particle generated by the incorporation of an *o*-nitrobenzyl containing network into a pH-responsive poly(methacrylic acid) (PMAA) particle matrix. Thus, the resulting particles differed from those having only photolabile units and from those having pH-responsive moieties. The preparation and controlled release properties of the particles were investigated with Fourier transform infrared (FTIR) spectroscopy, thermogravimetric analysis (TGA), dynamic light scattering (DLS), scanning electron microscopy (SEM), fluorescence spectroscopy, and fluorescence microscopy.

EXPERIMENTAL

Materials

2-Nitroacetophenone was purchased from Guangdong Wengjiang Chemical Reagent Co., Ltd. Nile red (NR) and methacryloyl chloride were provided by Shanghai Aladdin Chemistry Co., Ltd. Methacrylic acid (MAA), fluorescein diacetate (FDA), copper bromide ($CuBr_2$), 3-(4,5-dimethylazolyl-2)-2,5-diphenyltetrazolium bromide (MTT), and sodium borohydride were purchased from Energy Chemical. 2,2-Azobisisobutyronitrile (AIBN) was obtained from Shanghai Shanpu Chemistry Co., Ltd. Tetrahydrofuran (THF), triethylamine, dichloromethane, and acetonitrile (AN) were distilled over CaH_2.

Synthesis of 1-(2-Nitrophenyl)ethane-1,2-diyl Bis(2-methylacrylate) (NPEMA)

The following were prepared according to the methods provided in the Supporting Information: 2-bromo-1-(2-nitrophenyl) ethan-1-one, 2-(2-nitrophenyl)oxirane, and 1-(2-nitrophenyl)-1,2-ethanediol.

NPEMA was synthesized according to the literature.[12] Briefly, 1-(2-nitrophenyl)-1,2-ethanediol (0.50 g, 2.73 mmol) was dried through azeotropic distillation with dry THF thrice. Subsequently, freshly distilled THF (5 mL) and triethylamine (0.94 mL, 6.8 mmol) were added under N_2 at 0 °C. After 10 min of stirring, a solution of methylacryloyl chloride (0.66 mL, 6.8 mmol) in THF (3 mL) was added dropwise to the reaction mixture. The reaction mixture was stirred for approximately 2 h at room temperature, after which the reaction was quenched by the addition of an aqueous solution of $NaHCO_3$ (5%, 20 mL) and extracted with CH_2Cl_2 (3 × 30 mL). The organic layer was dried over anhydrous Na_2SO_4 for 24 h and concentrated. The crude product was purified by silica column chromatography to yield NPEMA (0.44 g, 51%) as a yellow oil.

^{1}H-NMR (δ, $CDCl_3$, Figure S3): 8.05–7.47 (m, 4H, Ar), 6.62–6.60 (m, 1H, CH), 6.23–6.09 (m, 2H, $=CH_2$), 5.58–5.67 (m, 2H, $=CH_2$), 4.57–4.68 (m, 1H, CH_2), 2.17 (s, 6H, CH_3).

Preparation of the Poly(methacrylic acid)–Poly[1-(2-nitrophenyl)ethane-1,2-diyl bis(2-methylacrylate)](PMAA–PNPEMA) Particles

Preparation of PMAA Particles without a Crosslinker. PMAA particles without a crosslinker were prepared by a method described elsewhere.[31] First, 0.495 mL of MAA was dissolved in 40 mL of absolute AN in a dry 50-mL, round-bottomed flask. Then, 16 mg of AIBN was added, and this was followed by 10 min of ultrasound. A fractionation device was attached to the flask, and then, the mixture was heated to 90 °C and stirred for 30 min. The original reaction temperature was maintained, and 20 mL of AN was distilled from the mixture. For the purification, the PMAA particles were obtained after four centrifugation steps (12,000 rpm) and washing with AN. The particles were dried at room temperature.

Preparation of the PMAA–PNPEMA Particles. The crosslinked PMAA–PNPEMA-coated particles {poly(methacrylic acid)/poly(methacrylic acid)–poly[1-(2-nitrophenyl)ethane-1,2-diyl bis(2-methylacrylate)](PMAA/PMAA–PNPEMA)} were prepared by a free-radical reaction. Briefly, 0.1 g of PMAA particles was dispersed in AN, and a certain amount of NPEMA (10, 20, and 40% of the weight of the monomers), 0.495 mL of MAA, and 16 mg of AIBN were added to the mixture. Then, the reaction was conducted with the same polymerization process mentioned previously. Finally, PMAA/PMAA–PNPEMA was dispersed in ethanol for 3 h to remove the uncrosslinked PMAA cores, and the obtained PMAA–PNPEMA particles were freeze-dried for 48 h and stored in the dark.

Measurements

The composition of the particles was determined with FTIR spectroscopy (Bruker, Tensor 27). TGA data were recorded on a thermogravimetric analyzer (TA, Q500) under a flowing nitrogen atmosphere at a heating rate of 20 °C/min from 100 to 650 °C. The surface morphology of the particles was characterized by SEM. The particle sizes were determined by DLS (Malvern, ZEN3600).

Preparation of the NR/FDA-Loaded PMAA–PNPEMA Particles

NR and FDA were used as fluorescent probes to assess the photo- and pH-controlled release behaviors. Typically, 2 mg of PMAA–PNPEMA particles was dispersed in 0.5 mL of NR or FDA solution in THF (0.4 mg/mL). This mixture was then oscillated with a vortex oscillator at room temperature for 30 s (5-s pulses with a 5-s delay) and then oscillated for 5 min without interruptions. The dispersion was centrifuged to collect NR- or FDA-loaded particles and washed with THF three times to remove the unloaded NR or FDA. After encapsulation, the NR-loaded particles were dried under N_2 overnight; this allowed

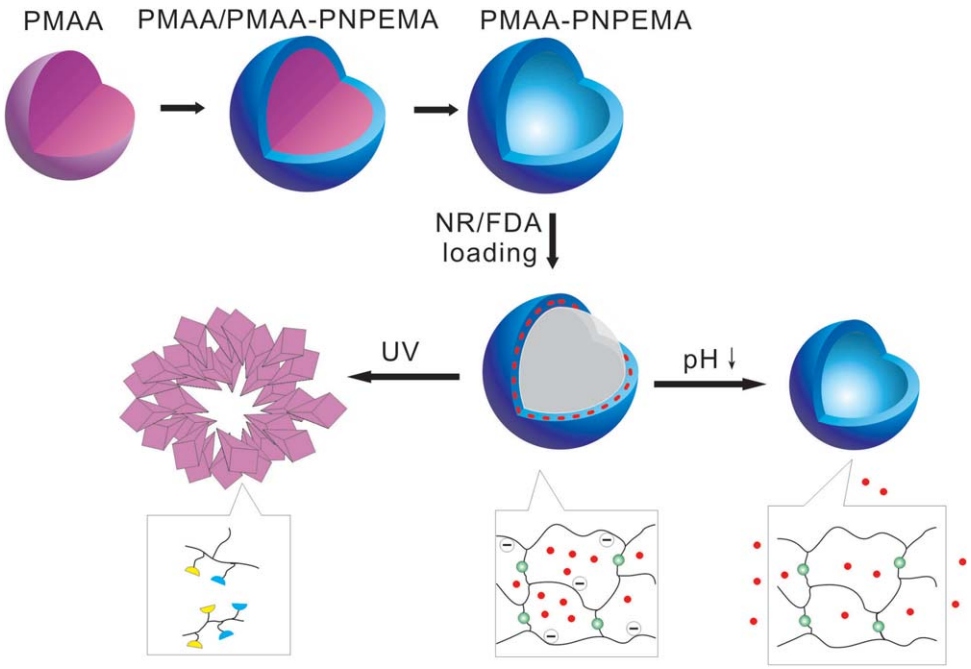

Figure 1. Schematic representation of photo/pH dual-responsive behaviors of the PMAA–PNPEMA particles. [Color figure can be viewed in the online issue, which is available at wileyonlinelibrary.com.]

THF to evaporate. FDA-loaded particles were dispersed in 0.5 mL of phosphate buffer solution (PBS; pH 7.4). Then, the aqueous solution was dialyzed against PBS with 1% dimethyl sulfoxide (DMSO) for 24 h. The medium was exchanged every 2 h to remove the THF and unloaded FDA. DMSO was removed through 1 day of dialysis against pure water.

pH-Triggered and Phototriggered NR-Release Study

To evaluate the pH-triggered release behavior of the encapsulated molecules, 2 mg of NR-loaded PMAA–PNPEMA particles were dispersed in 1 mL of medium with different pH values (4.4, 5.4, 6.5, and 7.4). Then, the fluorescence spectra of the mixture were monitored upon irradiation (365 nm, 5000 μW/cm^2) at an excitation wavelength of 557 nm with a fluorospectrophotometer (PerkinElmer, LS55).

In Vitro Cell Assays

Cell Culturing. Human uterine cervical cancer (HeLa) cells and SGC7901 cells were cultured in Roswell Park Memorial Institute medium 1640 supplemented with 10% fetal bovine serum and antibiotics (100 mg/mL streptomycin and 100 U/mL penicillin) at 37 °C with 5% CO_2.

***In Vitro* Cellular Uptake and FDA-Release Studies by Fluorescence Microscopy.** FDA, a nonfluorescent hydrophobic fluorescein derivative, was used to investigate the cellular uptake of the particles and the phototriggered release behaviors. FDA is not fluorescent when it is outside the cells or entrapped in particles because it cannot directly contact the esterases in the cell. However, fluorescein will be generated from FDA after release upon UV irradiation and hydrolysis by the intracellular esterases in cells.

The cellular uptake of FDA-loaded particles was studied with fluorescence microscopy. HeLa cells were seeded on six-well plates at a density of 6×10^4 cells per well. After 12 h of incubation at 37 °C, 20 μg/mL FDA-loaded particles were added and incubated for 6 h. The medium was removed, and the cells were rinsed twice with PBS buffer. Then, the cells were irradiated with 365-nm UV irradiation for 15 min, and this was followed by 2 h of incubation. Fluorescence images of the HeLa cells incubated with FDA-loaded particles with and without UV irradiation were taken with an inverted fluorescence microscope (Olympus IX-73) for different exposure times (50, 100, and 500 ms).

Particle Cytotoxicity Assay. The *in vitro* cytotoxicity of particles against SGC7901 cells was evaluated with MTT assay. First, SGC7901 cells were seeded in 96-well plates at a density of 1×10^5 cells/mL and incubated for 28 h. The cells were then treated with various amounts of particles (0–250 μg/mL). After incubation for 24 h or 48 h, MTT solution (0.5 mg/mL) was added to the wells, and the cells were incubated for 4 h at 37 °C. Next, 200 μL of DMSO was added to dissolve the formazan crystals. The absorbance of each well at 490 nm was measured with a microplate reader (Thermo, Multiskan GO). The cell viability was determined through a comparison of the absorbance of particle-incubated cells to that of control cells.

RESULTS AND DISCUSSION

Synthesis and Characterization of Photolabile Particles

Photolabile PMAA–PNPEMA particles designed as a triggered drug-delivery system are illustrated in Figure 1. First, the PMAA cores, which were soluble in methanol, were prepared as seeds. Then, the cores were coated with *o*-nitrobenzyl containing layers by a two-step radical polymerization to obtain PMAA/PMAA–PNPEMA particles. PMAA–PNPEMA particles were obtained by the dissolution of PMAA cores in ethanol. The drug could be

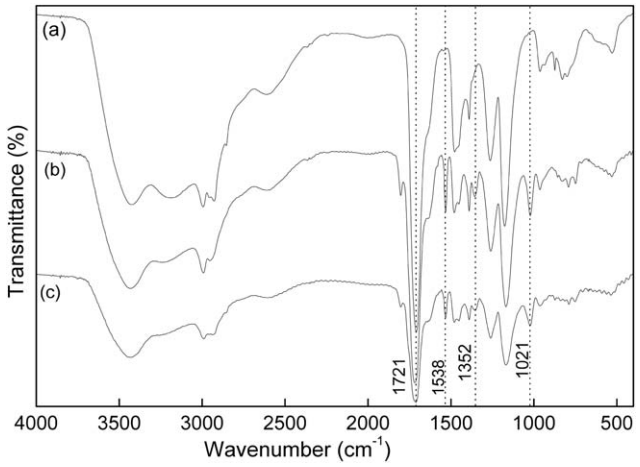

Figure 2. FTIR spectra of (a) PMAA, (b) PMAA/PMAA–PNPEMA, and (c) PMAA–PNPEMA-10%.

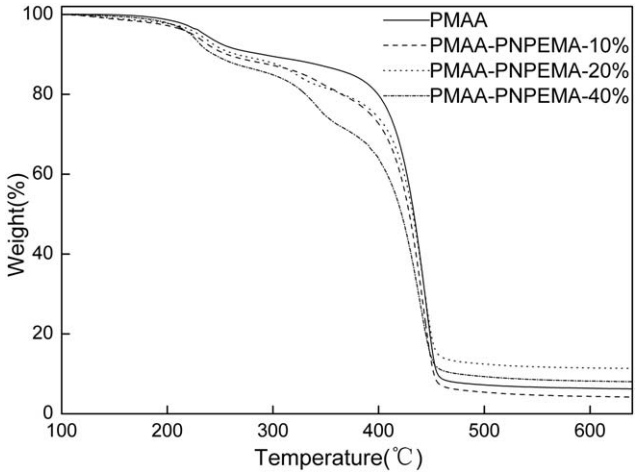

Figure 3. TGA thermograms of PMAA, PMAA–PNPEMA-10%, PMAA–PNPEMA-20%, and PMAA–PNPEMA-40%.

carried both in the cores and shells (Figure 1). Therefore, shells with a photolabile network could be degraded into short polymer chains, and the encapsulated molecules could be triggered and effectively released by UV irradiation.

The chemical formations of the particles (PMAA, PMAA/PMAA–PNPEMA, and PMAA–PNPEMA) were confirmed by FTIR spectra, as illustrated in Figure 2. The FTIR data showed strong peaks for C═O stretching vibrations at 1721 cm^{-1} attributed to PMAA, and the specific peaks for the —NO_2 (1538 and 1352 cm^{-1}), C═O (1803 cm^{-1}), and C—O—C (1021 cm^{-1}) of the NPEMA crosslinker were observed in the PMAA/PMAA–PNPEMA and PMAA–PNPEMA particles (Figure 2); this suggested that these two series of particles consisted of NPEMA crosslinker and MAA monomer. The specific peaks for MAA and NPEMA were observed in all of the samples with different crosslinker concentrations (see Figure S4 in the Supporting Information).

Furthermore, the structural differences of PMAA and PMAA–PNPEMA for different crosslinker concentrations (10, 20, and 40%) were also confirmed by the TGA data. As shown in Figure 3, compared with PMAA, PMAA–PNPEMA exhibited a lower pyrolysis temperature. Moreover, the pyrolysis temperature of PMAA–PNPEMA decreased as the crosslinking degree increased (Figure 3); this indicated that the crosslinked structure was not advantageous for the thermal stability of the copolymer. The particle size and surface morphology were then investigated with DLS and SEM, and typical results are shown in Table I and Figure 4(a). As shown Figure 4(a), the PMAA–PNPEMA particles a maintained good spherical morphology, although they were pretreated with methanol, which can cause collapse. The particle diameter was approximately 250–350 nm, as shown in the SEM image. The particle diameters of PMAA–PNPEMA with 10, 20, and 40% concentrations of the photolabile crosslinker NPEMA were 553, 295, and 804 nm, respectively (Table I).

Phototriggered Degradation of the PMAA–PNPEMA Particles

To verify the effect of external light on the PMAA–PNPEMA particles, the changes in the particles under mild photolysis conditions (365 nm, 5000 μW/cm^2) were investigated with FTIR spectroscopy, SEM, DLS, and absorption spectroscopy.

Figure 5 shows the UV-dependent changes in the FTIR spectra of the PMAA–PNPEMA particles. The typical peaks (1538 and 1352 cm^{-1}) of —NO_2 were reduced greatly, and new strong peaks for —NO at 1554 and 1012 cm^{-1} were generated upon UV irradiation. Moreover, after UV irradiation, the C═O stretching vibrations for the aromatic ketone at 1636 cm^{-1} became quite significant for the particles, and the peak at 1021 cm^{-1} for C—O—C redshifted to 1069 cm^{-1}; this suggested that carbonyl and carboxyl groups were generated by the breakage of the ester group. In addition, the conversion of the FTIR spectra for PMAA–PNPEMA-20% particles stored in an aqueous dispersion was detected after 2 days (Figure S5),and there were no significant changes. This also suggested that the

Table I. Average Particle Size Variation for the PMAA–PNPEMA Particles upon Photolysis (365 nm, 5000 μW/cm^2)

	Average particle size (nm)[a]			Polydispersity index[a]		
Sample	0 min of UV	2 min of UV	10 min of UV	0 min of UV	2 min of UV	10 min of UV
PMAA-PNPEMA-10%	553.1	707.0	242.7	0.319	0.537	0.539
PMAA-PNPEMA-20%	295.3	911.6	1217.0	0.219	0.663	0.800
PMAA-PNPEMA-40%	804.4	896.6	1050.0	0.271	0.305	0.788

The concentration of the PMAA–PNPEMA particle dispersions was 0.7 mg/mL.
[a] Determined by DLS in PBS (pH 7.4, 10 mM).

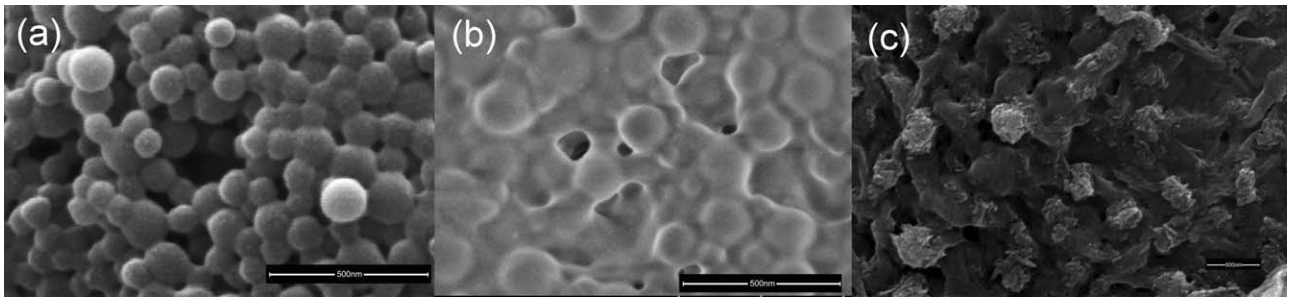

Figure 4. SEM images of the photoresponsive PMAA–PNPEMA-10% particles (a) before light irradiation, (b) after 2 min of light irradiation (365 nm, 5000 μW/cm^2), and (c) after 15 min of light irradiation (365 nm, 5000 μW/cm^2). The scale bars represent 500 nm. The concentration of the particle dispersions was 0.5 mg/mL.

hydrolysis for esters was not significant in aqueous dispersions. Figure 6 shows the absorption spectrum variations for the NPEMA crosslinker in AN and PMAA–PNPEMA-20% particles in aqueous dispersions. The absorption spectrum for the particles in aqueous dispersions was much different with the NPEMA crosslinker in AN because the the incident light was scattered by the dispersed particles. As shown in Figure 6(a), upon UV irradiation, the peaks at 260 nm weakened, and the appearance of the isosbestic points at 285 and 310 nm indicated the conversion of esters to carboxylic acid and ketone carbonyl group for NPEMA. As shown in Figure 6(b), the absorption spectrum change for nanoparticle dispersions (0.7 mg/mL) showed a remarkable redshift; this was consistent with the changes in the crosslinker upon UV exposure. Moreover, in comparison, the colorless transparent suspension became a light yellow suspension after 20 min of light irradiation (Figure S6, Supporting Information).

To further demonstrate that the PMAA–PNPEMA-10% particles were photodegradable, SEM images were obtained. As shown in Figure 4, the particles had spherical shapes, and the particle size distribution was relatively uniform before light activation. In contrast, obvious adhesion arose between the particles after 2 min of UV irradiation, and the particles were no longer spherical after 15 min of UV irradiation. SEM images for the PMAA–PNPEMA-20% and PMAA–PNPEMA-40% particles upon 10 min of UV irradiation were also detected, as shown in Figure 7. The spherical structure for the PMAA–PNPEMA-20% particles collapsed after 10 min of UV irradiation, and the particles changed into irregularly shaped small particles. However, for the PMAA–PNPEMA-40% particles, only partial destruction of the spherical structure was observed upon UV irradiation. These observations showed that the highly crosslinked samples were much more stable with UV irradiation. Particle size analysis indicated that light irradiation caused a volume expansion in the PMAA–PNPEMA-20%, and PMAA–PNPEMA-40% particles (Table I). This expansion may have been due to the rapid decrosslinking of particles upon UV irradiation. Figure S7 (Supporting Information) and Table I show the UV-dependent changes in the particle size of the PMAA–PNPEMA-10% particles. Notably, the particle size of PMAA–PNPEMA-10% increased after 1–2 min of UV irradiation and then decreased to about 243 nm upon 10 min of UV irradiation, and the polydispersity index value increased significantly upon UV irradiation. In the first 2 min of UV irradiation, the fracturing of crosslinks caused an expansion in volume. However, with increasing degradation degree after a relatively long period of UV exposure, the degradation product caused by the structural collapse settled down [Figure 4(c)]; this caused a decrease in the particle size. However, for the PMAA–PNPEMA-20% and PMAA–PNPEMA-40% particles, there was no obvious particle decline. These observations confirmed that the crosslinking degree was an important factor for the photosensitivity of the particles. These results indicate that the PMAA–PNPEMA particles were quite unstable upon UV irradiation. Therefore, such photoinduced degradation may ensure the viability of using PMAA–PNPEMA particles as an external stimuli-responsive drug-delivery system.

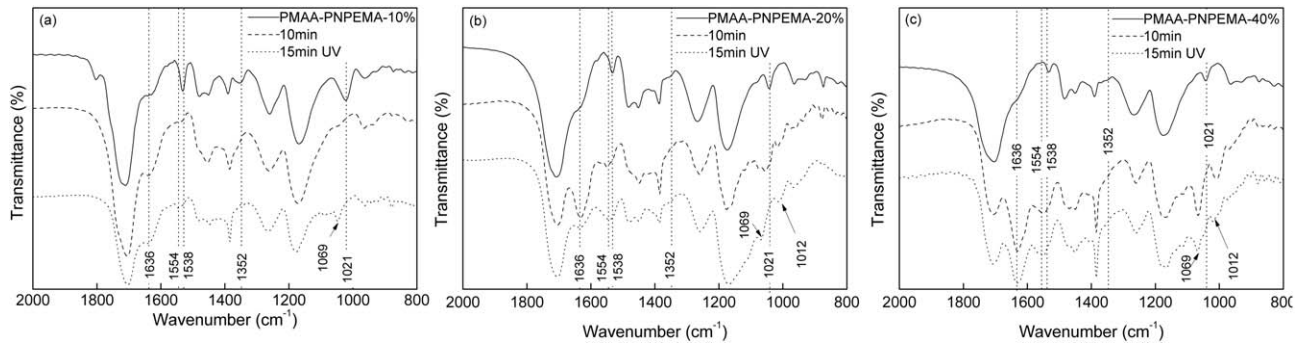

Figure 5. FTIR spectral variation for the (a) PMAA–PNPEMA-10%, (b) PMAA–PNPEMA-20%, and (c) PMAA–PNPEMA-40% particles upon photolysis (365 nm, 5000 μW/cm^2).

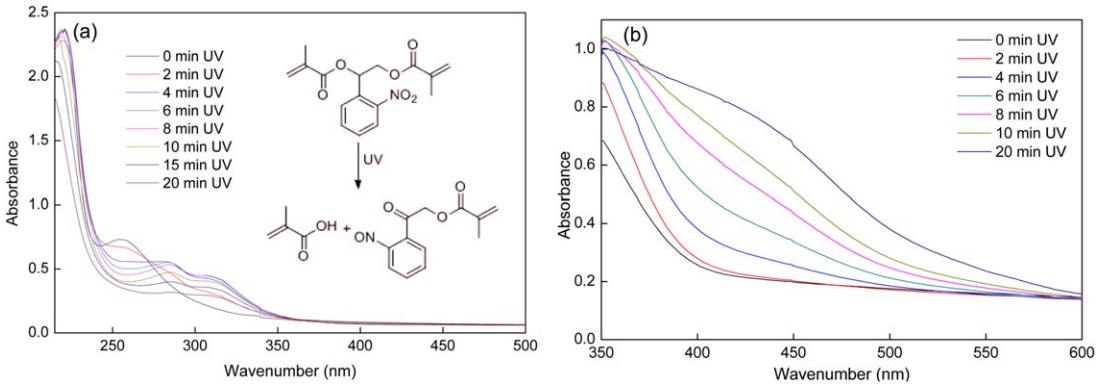

Figure 6. Absorbance spectra variation for the (a) NPEMA and (b) PMAA–PNPEMA-10% particles upon photolysis (365 nm, 5000 μW/cm^2). The concentration of the PMAA–PNPEMA-10% particle dispersions was 0.7 mg/mL. [Color figure can be viewed in the online issue, which is available at wileyonlinelibrary.com.]

In Vitro NR-Release Kinetics

To further assess the effect of the photocontrolled instability of the crosslinked PMAA–PNPEMA particles, light-triggered encapsulated molecule release was investigated with NR as the fluorescence probe. NR, a lipophilic fluorescent dye, displays obvious fluorescence activity in nonpolar media, and this fluorescence is quenched in aqueous environments (Figure S8, Supporting Information). As shown in Figure S8, in addition to having an 8-nm blueshift, the fluorescence spectrum for NR in the particles was similar to that of NR in acetone. Therefore, the efficiency of the triggered release was investigated with the solubility-dependent fluorescence emission, and the NR fluorescence intensity changed dramatically during the hydrophobic-to-hydrophilic transformation. The fluorescence intensity response of the NR-loaded PMAA–PNPEMA-10% aqueous dispersion after UV exposure at different pH values (4.4, 5.4, 6.5, and 7.4) is illustrated in Figure 8. Upon UV irradiation, a dramatic decrease in the fluorescence intensity was observed for the PMAA–PNPEMA-10% particles; this increase was ascribed to the transformation of the hydrophobic structure into a hydrophilic structure for the photolabile crosslinking and the increase in the particle size under mild UV irradiation. Furthermore, in the anionic network, the PMAA–PNPEMA particles were pH sensitive. The fluorescence intensity response to UV irradiation was evaluated under conditions with different pH values. As shown in Figure 9, 41, 49, and 61% of the fluorescence was quenched after 20 min of UV irradiation at pH 7.4, 6.5, and 5.4, respectively, whereas almost 77% of the fluorescence was quenched at pH 4.4; this suggested that the fluorescence response behavior of NR-loaded PMAA–PNPEMA-10% was pH dependent. At lower pH values, the protonation of the carboxylic acid enhanced the electrostatic repulsion between the

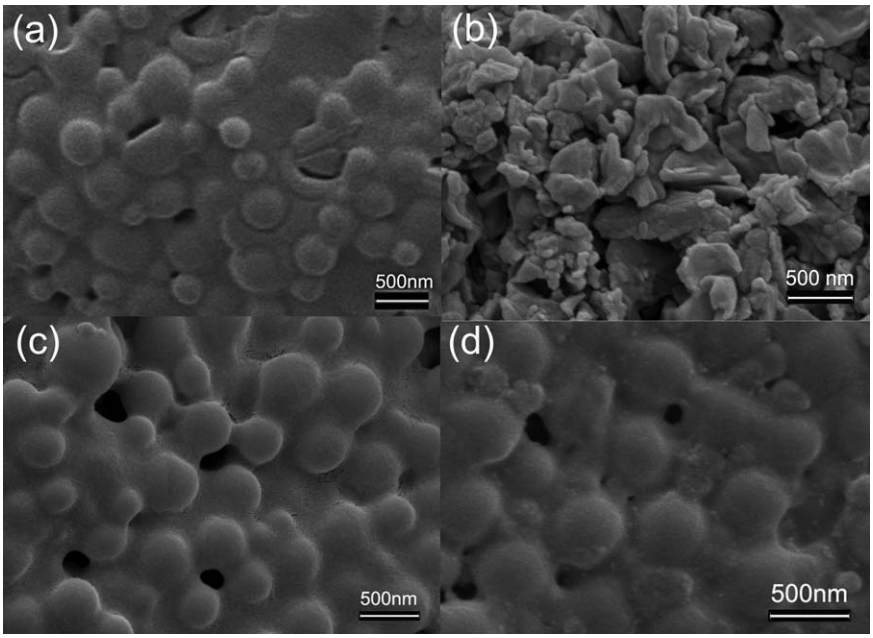

Figure 7. SEM images of the photoresponsive PMAA–PNPEMA-20% particles (a) before light irradiation and (b) after 10 min of light irradiation (365 nm, 5000 μW/cm^2) and photoresponsive PMAA–PNPEMA-40% particles (c) before light irradiation and (d) after 10 min of light irradiation (365 nm, 5000 μW/cm^2). The scale bars represent 500 nm.

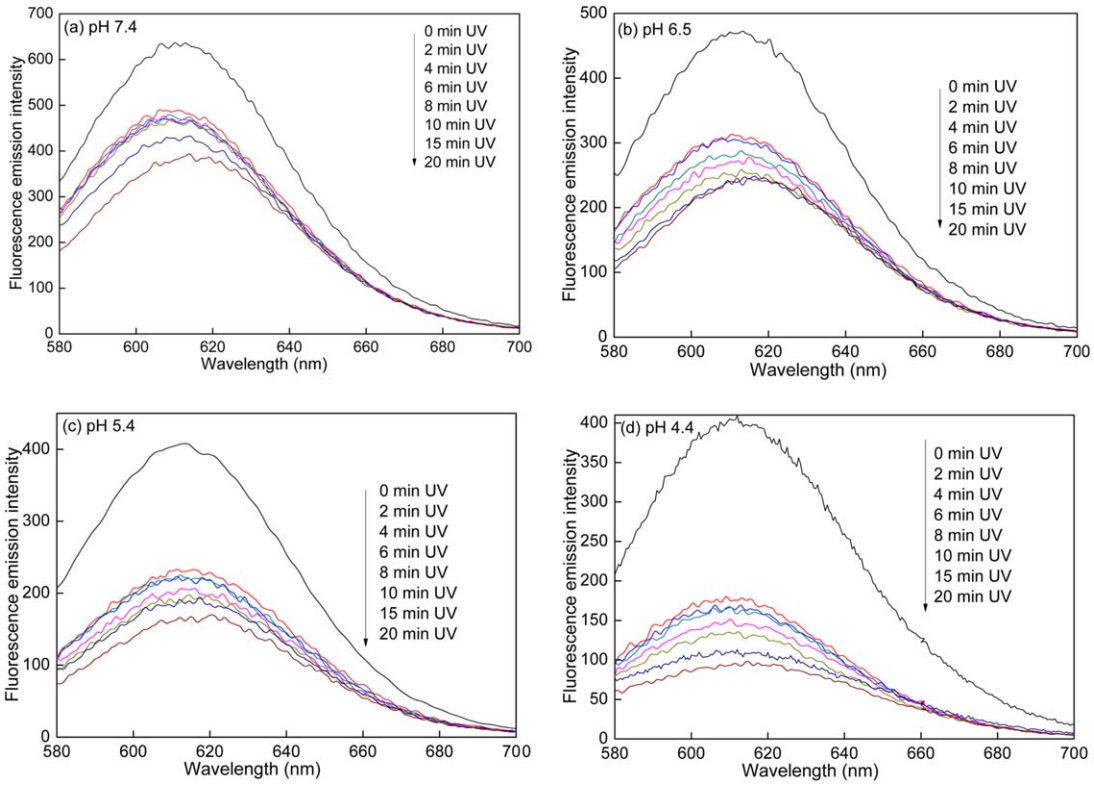

Figure 8. Fluorescence spectra of NR-loaded particles upon light irradiation (365 nm, 5000 μW/cm^2) with the excitation wavelength at 557 nm: (a) PMAA–PNPEMA-10% particles at pH 7.4, (b) PMAA–PNPEMA-10% particles at pH 6.5, (c) PMAA–PNPEMA-10% particles at pH 5.4, and (d) PMAA–PNPEMA-10% particles at pH 4.4.The concentration of the particle dispersions was 2 mg/mL. [Color figure can be viewed in the online issue, which is available at wileyonlinelibrary.com.]

network and the amino group in NR; this induced inducing an improvement in the NR-release rate from the particles. The effects on photocontrolled release for PMAA–PNPEMA-20% at different pH values were also evaluated, with similar results (Figures S9–S13, Supporting Information).

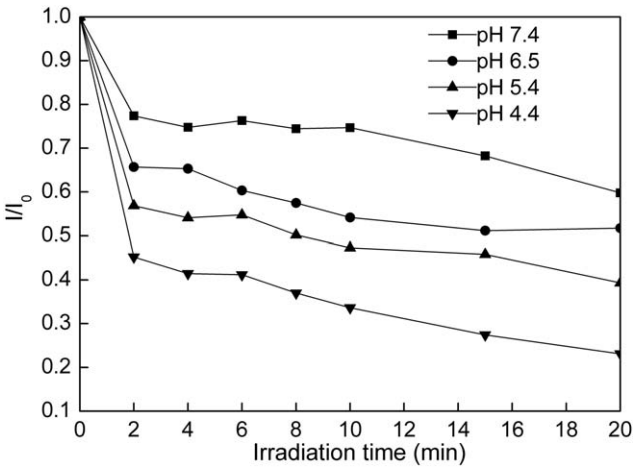

Figure 9. Plots of the normalized fluorescence intensity of NR at 614 nm versus the irradiation time (365 nm, 5000 μW/cm^2) for aqueous dispersions of photoresponsive PMAA–PNPEMA-10% particles with different pHs (4.4, 5.4, 6.5, and 7.4). The concentration of the particle dispersions was 2 mg/mL. I/I_0 = normalized fluorescence

In Vitro Cell Assays

The SGC7901 cells were incubated with various concentrations (0–250 μg/mL) of PMAA–PNPEMA-10% particles for 24 and 48 h to assess the toxicity and biocompatibility of the particles. As shown in Figure 10 and Figure S14 (Supporting Information), there was no significant change in the cell viability over the range of concentrations up to 250 μg/mL. In addition, no

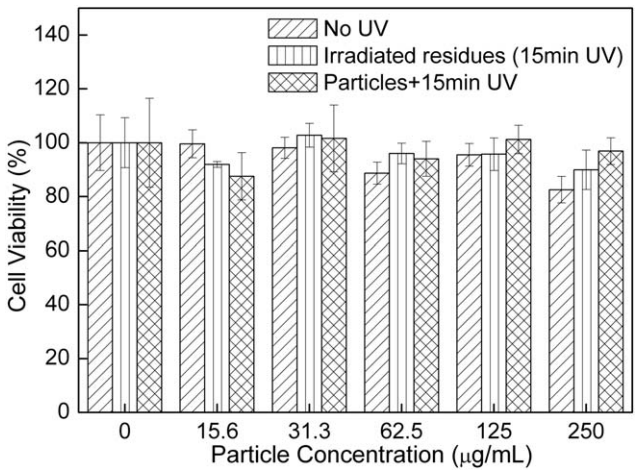

Figure 10. Cell survival assay of the SGC7901 cells exposed to PMAA–PNPEMA-10% particles (with dosages ranging from 0 to 250 μg/mL) for 24 h. Data are shown as means and standard deviations ($n = 4$).

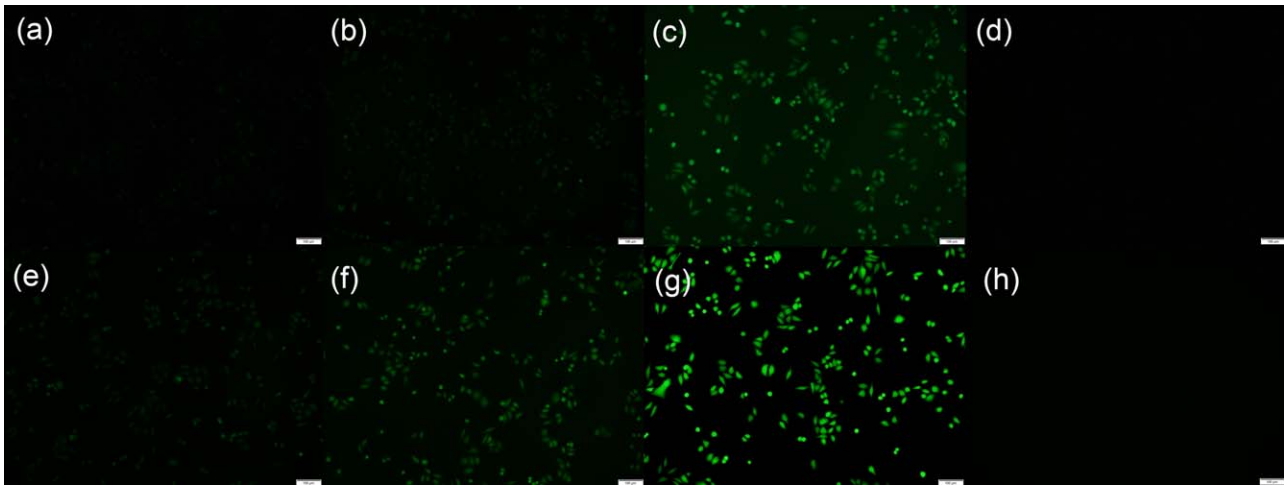

Figure 11. Intracellular FDA release from the FDA-loaded PMAA–PNPEMA-10% particles and PMAA particles evaluated by fluorescence microscopy against HeLa cells before or after 10 min of light irradiation: (a–c) FDA-loaded PMAA–PNPEMA-10% particles without light irradiation with exposure times of 50, 100, and 500 ms, respectively; (d) FDA-loaded PMAA particles without light irradiation with a 100-ms exposure time; (e–g) FDA-loaded PMAA–PNPEMA-10% particles upon 10 min of light irradiation with exposure times of 50, 100, and 500 ms, respectively; and (h) FDA-loaded PMAA particles upon 10 min of light irradiation with a 100-ms exposure time. The concentration of the particles was 20 μg/mL. The wells were washed with PBS three times to remove the unswallowed particles after particle incubation for 6 h at 37 °C. The cells were irradiated with a UV lamp at 365 nm (5000 μW/cm^2) for 15 min. The scale bars represent 100 μm. [Color figure can be viewed in the online issue, which is available at wileyonlinelibrary.com.]

signs of toxicity were observed for cells incubated with the irradiated residues of the UV-degraded products of PMAA–PNPEMA-10%, and the cell viability did not change observably upon exposure to 15 min of UV irradiation. The results confirm the good biocompatibility of PMAA–PNPEMA-10% and its irradiated residues.

It was anticipated that PMAA–PNPEMA particles would disintegrate at lower pH values upon exposure to UV irradiation. To further confirm this idea, the release of the intracellular encapsulated molecules from the particles was evaluated by fluorescence microscopy with HeLa cells. FDA was entrapped in the PMAA–PNPEMA particles as a model fluorophore because the nonfluorescent FDA could be transformed into highly fluorescent fluorescein by intracellular esterases. Nanoparticle cell uptake and phototriggered FDA release from the PMAA–PNPEMA particles in the cells were confirmed by the fluorescence of fluorescein (Figure 11). Figure 11(a–c,e–g) shows the fluorescence images of the HeLa cells incubated with the FDA-loaded PMAA–PNPEMA-10% particles before and after 15 min of UV activation with different exposure times. The mean fluorescence intensities of the cells incubated with FDA-loaded particles for 50-, 100-, and 500-ms exposure times were relatively low; this indicated that only a small amount of FDA leaked out from the particles into the cells. As expected, obvious green fluorescence was found after just 15 min of light activation, as shown in Figure 11(e–g). As illustrated in Figure 11, compared with the PMAA–PNPEMA particles, the cells incubated with FDA-loaded PMAA particles before or after 15 min of UV activation with the 100-ms exposure time showed no obvious fluorescence; this indicated that FDA could not be released from the PMAA particles even after UV irradiation.

CONCLUSIONS

In summary, novel dual-responsive (light and pH) biocompatible PMAA-based particles (PMAA–PNPEMA) were developed successfully. The structures and properties of the PMAA–PNPEMA particles with a photolabile network were characterized by FTIR spectroscopy, DLS, SEM, and TGA. We verified that the PMAA–PNPEMA particles could rupture and release the encapsulated contents efficiently upon light irradiation at a low pH level. The photoswitching of the PMAA–PNPEMA particles was confirmed by SEM, fluorescence spectroscopy, and DLS. Intracellular drug delivery was investigated to demonstrate that the FDA-release behavior in cells was light dependent.

ACKNOWLEDGMENTS

This work was financially supported by the National Natural Science Foundation of China (contract grant number 81302706), the State Key Laboratory of Natural and Biomimetic Drugs (contract grant number K20120212), and the Scientific Research Program of the Shaanxi Provincial Education Department (contract grant number 2013JK0759).

REFERENCES

1. Klinger, D.; Landfester, K. *Macromolecules* **2011**, *44*, 9758.
2. Basak, D.; Ghosh, S. *ACS Macro Lett.* **2013**, *2*, 799.
3. Al-Nahain, A.; Lee, S. Y.; In, I.; Lee, K. D.; Park, S. Y. *Int. J. Pharm.* **2013**, *450*, 208.
4. Wilson, J. T.; Keller, S.; Manganiello, M. J.; Cheng, C.; Lee, C.-C.; Opara, C.; Convertine, A.; Stayton, P. S. *ACS Nano* **2013**, *7*, 3912.

5. Bhargava, P.; Tu, Y.; Zheng, J. X.; Xiong, H.; Quirk, R. P.; Cheng, S. Z. *J. Am. Chem. Soc.* **2007**, *129*, 1113.
6. Sugihara, S.; Hashimoto, K.; Okabe, S.; Shibayama, M.; Kanaoka, S.; Aoshima, S. *Macromolecules* **2004**, *37*, 336.
7. Dai, F.; Sun, P.; Liu, Y.; Liu, W. *Biomaterials* **2010**, *31*, 559.
8. Guerry, A.; Cottaz, S.; Fleury, E.; Bernard, J.; Halila, S. *Carbohydr. Polym.* **2014**, *112*, 746.
9. Qiu, F.; Wang, D.; Zhu, Q.; Zhu, L.; Tong, G.; Lu, Y.; Yan, D.; Zhu, X. *Biomacromolecules* **2014**, *15*, 1355.
10. Xuan, J.; Han, D.; Xia, H.; Zhao, Y. *Langmuir* **2014**, *30*, 410.
11. Rao, J.; Khan, A. *J. Am. Chem. Soc.* **2013**, *135*, 14056.
12. Yu, L.; Lv, C.; Wu, L.; Tung, C.; Lv, W.; Li, Z.; Tang, X. *Photochem. Photobiol.* **2011**, *87*, 646.
13. Rabnawaz, M.; Liu, G. *Macromolecules* **2012**, *45*, 5586.
14. Wang, Z.; Yu, L.; Lv, C.; Wang, P.; Chen, Y.; Tang, X. *Photochem. Photobiol.* **2013**, *89*, 552.
15. Lv, C.; Wang, Z.; Wang, P.; Tang, X. *Langmuir* **2012**, *28*, 9387.
16. Lee, J. H.; Kim, J.-C. J. *Ind. Eng. Chem.* **2014**, *20*, 3075.
17. Tian, Y.; Kong, Y.; Li, X.; Wu, J.; Ko, A. C. T.; Xing, M. *Colloids Surf. B* **2015**, *134*, 147.
18. Yu, H.; Cui, Z.; Yu, P.; Guo, C.; Feng, B.; Jiang, T.; Wang, S.; Yin, Q.; Zhong, D.; Yang, X.; Zhang, Z.; Li, Y. *Adv. Funct. Mater.* **2015**, *25*, 2489.
19. Wang, G.; Dong, J.; Yuan, T.; Zhang, J.; Wang, L.; Wang, H. *Macromol. Biosci.* **2016**, to appear.
20. Meng, L.; Huang, W.; Wang, D.; Huang, X.; Zhu, X.; Yan, D. *Biomacromolecules* **2013**, *14*, 2601.
21. Li, Y.; Xiao, W.; Xiao, K.; Berti, L.; Luo, J.; Tseng, H. P.; Fung, G.; Lam, K. S. *Angew. Chem. Int. Ed.* **2012**, *51*, 2864.
22. Shao, Y.; Shi, C.; Xu, G.; Guo, D.; Luo, J. *ACS Appl. Mater. Interfaces* **2014**, *6*, 10381.
23. Sokolovskaya, E.; Rahmani, S.; Misra, A. C.; Bräse, S.; Lahann, J. *ACS Appl. Mater. Interfaces* **2015**, *7*, 9744.
24. García-Juan, H.; Nogales, A.; Blasco, E.; Martínez, J. C.; Šics, I.; Ezquerra, T. A.; Piñol, M.; Oriol, L. *Eur. Polym. J.* **2015**, to appear.
25. Li, J.; Yu, Z.; Jiang, H.; Zou, G.; Zhang, Q. *Mater. Chem. Phys.* **2012**, *136*, 219.
26. Yan, B.; Boyer, J.-C.; Branda, N. R.; Zhao, Y. *J. Am. Chem. Soc.* **2011**, *133*, 19714.
27. Jiang, J.; Tong, X.; Zhao, Y. *J. Am. Chem. Soc.* **2005**, *127*, 8290.
28. Babin, J.; Pelletier, M.; Lepage, M.; Allard, J. F.; Morris, D.; Zhao, Y. *Angew. Chem. Int. Ed.* **2009**, *48*, 3329.
29. Gohy, J. F.; Zhao, Y. *Chem. Soc. Rev.* **2013**, *42*, 7117.
30. Murthy, N.; Thng, Y. X.; Schuck, S.; Xu, M. C.; Fréchet, J. M. J. *J. Am. Chem. Soc.* **2002**, *124*, 12398.
31. Yang, P.; Li, D.; Jin, S.; Ding, J.; Guo, J.; Shi, W.; Wang, C. *Biomaterials* **2014**, *35*, 2079.